ELSEVIER

Journal of Fluids and Structures 26 (2010) 503–516

JOURNAL OF FLUIDS AND STRUCTURES

www.elsevier.com/locate/jfs

Structural analysis of aquaculture net cages in current

H. Moe[a,b,*], A. Fredheim[a], O.S. Hopperstad[b]

[a]*SINTEF Fisheries and Aquaculture, No-7465 Trondheim, Norway*
[b]*Structural Impact Laboratory (SIMLab), Centre for Research-Based Innovation, Department of Structural Engineering, Norwegian University of Science and Technology (NTNU), No-7491 Trondheim, Norway*

Received 11 December 2008; accepted 27 January 2010
Available online 5 March 2010

Abstract

A method for structural analysis of aquaculture net cages has been developed and verified for a netting solidity of 0.23, water current velocities from 0.1 to 0.5 m/s and relatively large deformations (volume reduction up to 70%) by comparing the numerical results to tests in a flume tank. Strength analysis was performed using commercial explicit finite element software to calculate distribution of loads in the net cage due to current, weights and gravity. The net cage was modelled using truss elements that represented several parallel twines. Sub-elements allowed the trusses to buckle in compression, and only negligible compressive forces were seen in the numerical results. Resulting drag loads and cage volume were shown to be dependent on the net cage size and weight system. Drag loads increased almost proportional to the current velocity for velocities in the range of 0.2–0.5 m/s, while the cage volume was reduced proportional to the current velocity. The calculated forces in ropes and netting of full-size net cages were well below the design capacity for current velocities up to 0.5 m/s. However, netting seams in the bottom panel of the net cage were identified as a potential problem area as the forces could reach the design capacity.

Keywords: Non-linear structural analysis; Net cages; Explicit finite element analysis; Model tests; Loads from water current; Morison's equation

1. Introduction

Net cages for aquaculture have traditionally been dimensioned and produced based on empirical data (Standards Norway, 2003). However, the requirements for documentation of net cage strength and volume increase, and the need for development of methods for structural analysis arises. In addition, fish farming is developing outside the borders of experience. The size of net cages increases rapidly, reaching volumes above current experience. More exposed locations are used for fish production, introducing higher loads on the net cage and fish farm from strong water currents and large waves. Strength analysis can also be a useful tool for development of net cage designs (Moe et al., 2005) to avoid escape of fish and ensure sufficient volume for good fish welfare and water quality.

It is not straightforward to analyze a fish farm or a single net cage (Fig. 1). The loads acting on the structure will be the result of a fluid-structure interaction between moving sea-water and the deformed net. Analyses of net cages involve a high degree of non-linearity, both in loads, deformation and sometimes also material properties. In addition, loads from waves and

*Corresponding author at: SINTEF Fisheries and Aquaculture, No-7465 Trondheim, Norway. Tel.: +47 4000 5350; fax: +47 932 70 701.
E-mail address: Heidi.Moe@Sintef.no (H. Moe).

0889-9746/$ - see front matter © 2010 Elsevier Ltd. All rights reserved.
doi:10.1016/j.jfluidstructs.2010.01.007

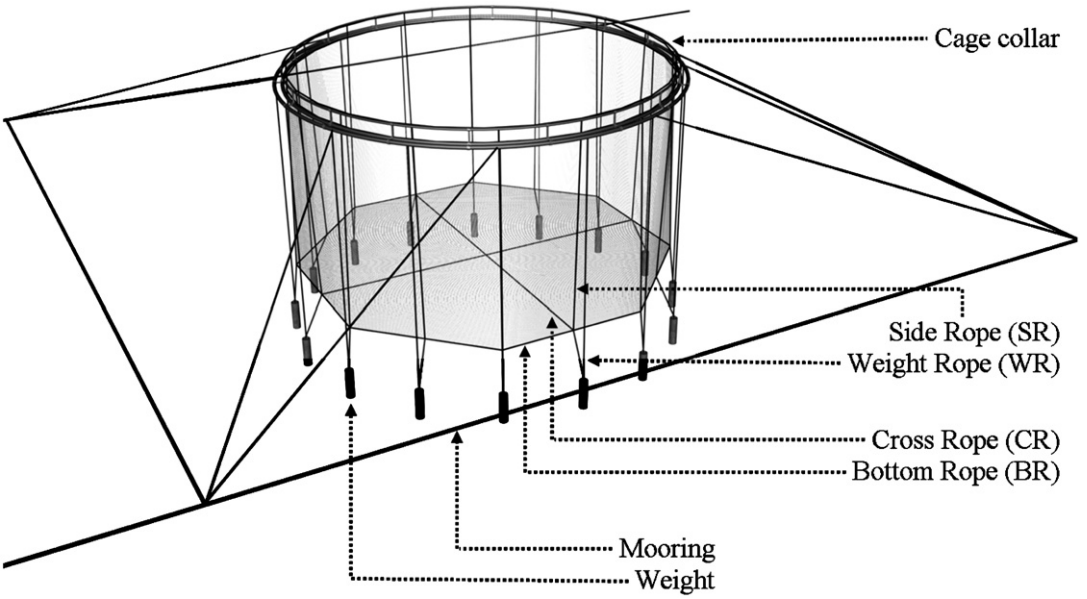

Fig. 1. Illustration of traditional circular fish cage.

current, damping and inertia loads are complex to model for netting materials in a general Finite Element Analysis (FEA) program, while programs with appropriate load modules often have shortcomings in the structural model. An analysis involving a complete fluid and structure interaction model (CFD and FEA) will be complex and extremely demanding on computational resources, and to our knowledge attempts to perform such analysis on net cages have not been performed. There is ongoing work to verify and develop CFD methods for flow around net structures. This work reveals the complexity of such flows and the need of new knowledge and methods (Klebert, 2009; Enerhaug and Lader, 2009) Thus, the only current option is to use methods to calculate loads from moving fluids on netting structures, such as Morison's equation or equations based on tank test results (Løland, 1991). However, both these methods currently have limitations concerning amongst other the solidity of the net panel (ratio between area of netting material and total area), deformations and current velocity.

In the literature, net structures have been modelled using truss, beam, cable or spring elements to represent the twines (Fredheim, 2005; Gignoux and Messier, 1999; Li et al., 2006; Huang et al., 2006; Zhan et al., 2006; Zhao et al., 2007), or using 2-D membrane elements (Lader and Fredheim, 2006; Tsukrov et al., 2003; Priour, 1999; Tronstad, 2000). The previous work included custom made software and/or elements, and focused on the hydrodynamics and displacements rather than the distribution of loads in the model. Our approach to structural analyses was to apply a commercial FEA software, which could include various material models and ensure effective modelling, processing and post-processing. In this work, truss elements were applied to model the net cage. The fact that netting and ropes do not take compression was modelled by introducing sub-elements, which combined with an explicit finite element code allowed the elements to buckle in compression.

Due to the mentioned limitations in methods for structural analysis of net cages, it is important to validate the methods applied, for instance by comparing results with model tests. The first step will be a static load situation involving a constant and uniform current. This paper presents a method for numerical strength analysis of net cages in constant uniform current verified for limited solidity, deformations and current velocities, applying Morison's equation to calculate loads on the deformed net cage. The model was validated by comparing the results to model tests of a cage without bottom performed in a flume tank (Lader and Enerhaug, 2005), and then the method was applied to study deformations and global and internal forces of full-scale net cages in uniform current.

2. Materials and methods

2.1. Analysis and modelling

Strength analyses were performed using the finite element method software ABAQUS Explicit (Dessault Systèmes, 2007; Moe et al., 2005). A large number of degrees of freedom were required to model the complete geometry of a

full-scale net cage. In practice, it was not possible to analyze a model of a standard size net cage including all twines. Thus, major model simplifications had to be performed to reduce the computation time to an acceptable level. The applied square mesh Raschel knitted netting, made out of very thin Nylon (PA6) filaments, had a negligible bending stiffness (Klust, 1982). The net cage model was therefore built up of 3-D truss elements (Dessault Systèmes, 2007) and each truss element represented several parallel twines in the netting. The truss elements were given the combined properties of the represented twines, i.e. the cross-section area of the truss element was equal to the sum of the cross-section area of the represented twines. The applied netting materials did not carry compressive loads. Therefore, each global truss element was divided into at least two sub-elements, allowing the twines to buckle when subjected to compression. Only negligible compressive loads were seen in the numerical results.

Three different models, described in Table 1, were analysed. Model M1 was similar to the cage without bottom subjected to model tests in a flume tank. Twine thickness, t, and half mesh width $w_{1/2}$ (ISO, 2002) were increased by approximately 8% compared with given values in Lader and Enerhaug (2005) in order to account for expansion due to water absorption (Moe et al, 2007). The solidity was calculated as $Sn = 2t/w_{1/2}$. For all models, the netting dimensions were equal to typical smolt nets (for juvenile salmon). M1 was modelled with one truss for each fourth twine. This model was also analyzed using a detailed mesh with one truss for each twine to verify the model simplification (for one load case, Fig. 2). This refinement resulted in drag and lift forces less than 0.7% different to the results using the coarser mesh (four twines per truss). Two full-scale models (Fig. 3) represented a cage of standard industry size a few years ago (M2), and a large cage according to present industry standards (M3). M2 and M3 had 80 and 128 elements around the circumference, which should be sufficient to capture the global deformations in the net cage. In comparison, M1 had 63 elements along the circumference, which was proved to be sufficient.

The full-scale models, M2 and M3, had 16 and 32 side ropes and 4 and 8 cross ropes, respectively, in addition to main and bottom ropes (Fig. 1). M1 consisted of netting only.

The strains in the netting were in general small (less than 10%), and a linear elastic material model was applied for all analyses (Moe et al., 2007, in press). The stiffness of the netting material was chosen as 82 MPa, given for a specified pretension in Moe et al. (2007). This simplified netting material model was found sufficient for these global analyses (see Section 4). However, boundary conditions and load cases that induce large strains in the netting would require a more refined material model. Ropes were given a stiffness of 1 GPa (Moe et al., 2005) and a diameter of 18 mm. The

Table 1
Model dimensions.

Model	Circumference (m)	Cage depth (m)	Twine thickness, t (mm)	Half mesh width, $w_{1/2}$ (mm)	Solidity, Sn	Truss length (mm)	Twines pr. truss
M1	4.42	1.41	2	17.6	0.23	70.4	4
M2	90	20	2	16	0.25	1125	70.3
M3	160	40	2	16	0.25	1250	78.1

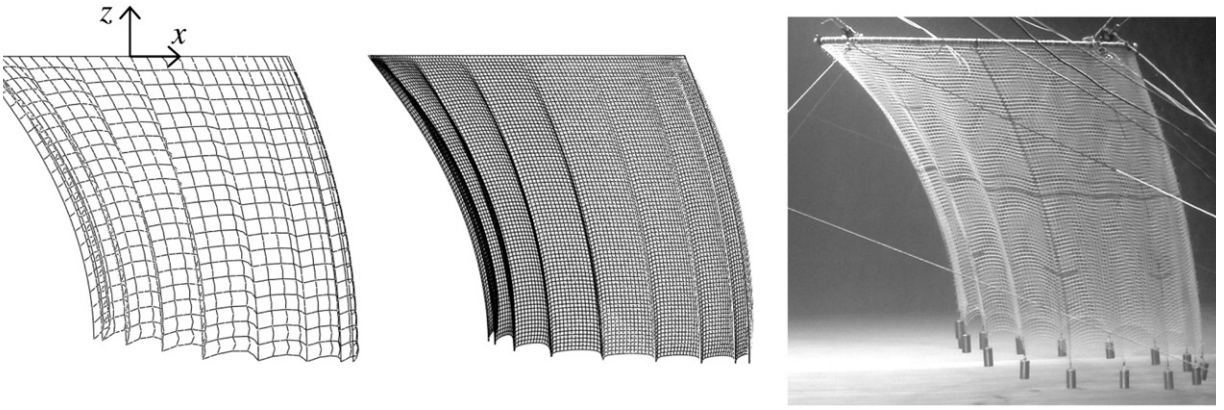

Fig. 2. Comparison of deformed shape from numerical models with applied (coarse) and detailed mesh and physical model of M1 (16 weights of 800 g and current velocity of 0.34).

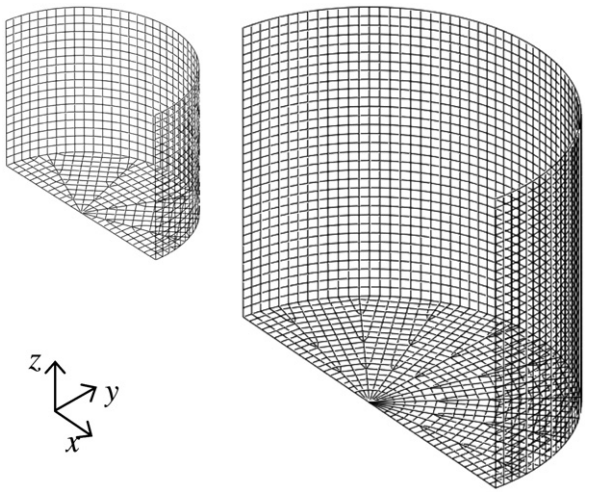

Fig. 3. Models M2 and M3. The relative difference in size is maintained in the figure, which shows half of each model.

bottom of the full-scale net cages consisted of 8 and 16 netting triangles for M2 and M3, respectively. These were joined by seams that were assumed to have a constant stiffness equal to ten parallel twines (seam cross-section area was 10 times the area of one twine). Both netting and ropes are close to neutrally buoyant in water, and both materials were given a density of 1125 kg/m^3 (density of water was given as 1025 kg/m^3).

The net cage volume was estimated by dividing the net cage into sections and summing their approximate volumes. M1, M2 and M3 were divided into 21, 19 and 33 sections over their depth (the possible volume below the bottom rope was not considered). For the unloaded cage configuration the sections were horizontal, circular disks with a thickness equal to the truss length (except the upper and lower sections, which were half as thick). The volume of a deformed section was calculated as the horizontal cross-section multiplied by the average (vertical) thickness of the section circumference.

2.2. Boundary conditions and loads

The net cage of a circular fish cage (Fig. 1) is usually attached to the cage collar at each side rope. In order to get the correct boundary conditions of the net cage, both the bending stiffness of the cage collar and the tensile stiffness of the mooring lines should be modelled. However, for simplicity, neither the cage collar nor the mooring system was modelled in these analyses, but assumed to keep their original shape and position, although this may affect the distribution of loads in the net cage (see Section 4). For M1, both the tank test model and the numerical model were attached to a rigid cage collar over the full circumference, consequently with no effect of mooring stiffness on the net cage response in current. The full-scale models, M2 and M3, were assumed attached to a rigid cage collar at all side ropes, which were 16 and 32, respectively.

In the numerical analysis, loads from current, weights and gravity were applied gradually to ensure that external work was converted to internal energy without introducing significant kinetic or viscous energy. The numerical models were subjected to loads representing a uniformly distributed current with constant velocity, $\mathbf{U}$, acting in the x-direction (coordinate system defined in Figs. 2 and 3). The cross-flow principle was applied (Hoerner, 1965), assuming that the current could be separated into flow tangential and normal to the element axis. The first step in the current load calculation for an element was to decompose $\mathbf{U}$ into tangential and normal velocity components, $\mathbf{U}_T$ and $\mathbf{U}_N$, as shown for an element in the xz-plane in Fig. 4. However, most elements were oriented in the xyz-space and subjected to three-dimensional velocity vectors. Each truss element was considered as individual, friction-free cylinders, and tangential force was ignored. The resulting load acting on each truss element was the normal load, $\mathbf{F}_N$, calculated using the drag term of Morison's equation (Faltinsen, 1990):

$$\mathbf{F}_N = \tfrac{1}{2}\rho C_D A_p |\mathbf{U}_N| \mathbf{U}_N, \tag{1}$$

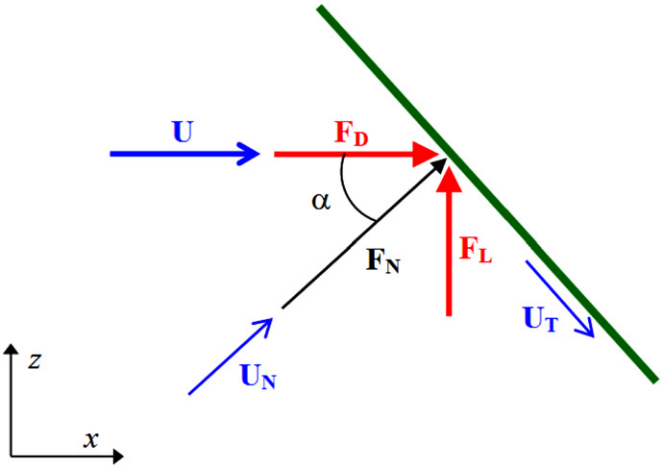

Fig. 4. Calculation of current loads for an element in the xz-plane.

where $\rho = 1025\,\mathrm{kg/m^3}$ (density of seawater) and C_D is the drag coefficient. A_p is the projected area of the truss element, which is the sum of the projected area for all twines represented by the truss element. $A_p = ndL$, where n is number of twines represented by the truss, d the twine diameter and L the truss length. $\mathbf{F}_N$ was decomposed in the x-, y- and z-directions and applied as concentrated loads in adjacent nodes. Drag load ($\mathbf{F}_D$) and lift load ($\mathbf{F}_L$) were found as the x and z components of $\mathbf{F}_N$, respectively.

During the model tests, total lift and drag forces were found as the sum of the reaction forces in eight mooring lines attached to the rigid cage collar (steel ring). The model was submerged, allowing for measurement of lift, and the effect of the steel ring was subtracted from the resulting drag and lift force measurements. In the numerical analysis, the resulting drag and lift forces were calculated by summing up the loads calculated for each truss element (Eq. (1)).

For M1, it was assumed that the current velocity was reduced by 20% after passing the first net wall (Lader and Enerhaug, 2005). For the full size cages the velocity reduction was assumed to be 15%, corresponding to findings by Løland (1991). The bottom would in general experience a high degree of shadow effects, as parts of the bottom would be close to horizontal (see Section 4), and the current velocity was thus reduced by 50% in the (initially horizontal) bottom. A sensitivity study comparing physical tests and numerical analysis of net cages with and without a bottom panel would be required to establish a more accurate drag coefficient for the bottom panel.

Fredheim (2005) presented results implying that the drag term of Morison's equation could be applied with a constant drag coefficient to calculate drag on netting for a limited range of Reynolds number and solidities (less than 0.25). M1, M2 and M3 were analysed for current velocities ranging from 0.1 to 0.5 m/s, corresponding to Reynolds number $\mathrm{Re} \in [174\text{–}870]$ ($\mathrm{Re} = Ud/\nu$, where ν is the kinematic viscosity, $\nu = 1.15 \times 10^{-6}\,\mathrm{m^2/s}$ for seawater). Based on findings in Fredheim (2005), the drag coefficient was given a constant value $C_D = 1.15$ (valid for the applied solidities, Table 1, and given range of Reynolds number).

Net cage structures are highly flexible and will experience large displacements when subjected to currents. The displacements are dependent on current loads, and the direction and magnitude of current forces are affected by the net cage displacements. An iteration scheme was applied to account for this complex relationship. First, current forces were calculated based on the initial (unloaded) cage geometry and the resulting deformations of the cage model were found. New loads were calculated based on the deformed model, resulting in a new cage configuration. The last step was repeated until the difference in drag and lift was less then 2% between the last two iterations (most often the difference was less than 1%). The whole process was run by a custom made automatic MATLAB routine, which calculated the forces, ran ABAQUS, extracted output from the FEA analysis and started a new iteration if convergence was not reached. The number of iterations varied from 2 to 6 for low to high current velocities.

M1 was analyzed using four different bottom weight configurations: 16 weights of 400, 600 and 800 g (3.0, 4.5 and 6.0 N submerged weight) and 4 weights of 6.0 N. The weights were attached directly to the netting and equally distributed along the circumference. M2 was subjected to a concentrated load of 1000 N at the end of each side rope, while M3 was analyzed for both 1000 and 2000 N at all 32 side ropes. Both M2 and M3 were subjected to a weight of 1000 N at the centre of the bottom.

3. Results

3.1. Comparison of numerical analyses and model tests

M1 was analyzed for various weight configurations and current velocities corresponding to load cases presented in Lader and Enerhaug (2005), who performed physical model tests of M1 at the North Sea Centre flume tank in Denmark. The results from the numerical analyses of M1 were compared to the physical model tests.

Fig. 5 shows a selection of 2-D plots of the deformed shape from the various analyzed load cases compared with the configuration in calm water (dotted lines). The 2-D positions of the physical model were measured at 8 points (front, aft and centre of net cage) as indicated in Fig. 5 using a video system. The overall impression from these figures was that the deformed shapes achieved from numerical analyses corresponded very well to the shapes of the physical model. It was noted that the tank test model had an initially imperfect geometry (slightly skew in calm water, as shown in Fig. 5), that must be assumed had an effect on deformation and loads in current. The bottom circumference of the physical model was significantly smaller than the upper circumference, which was not the case in the numerical model. This was a consequence of the design of the joint between two twines (not included in the FE model), which makes unloaded netting contract. The vertical deformation of the net was slightly larger in the numerical analyses for cages with large deformations (16×400 g, $v_c = 0.56$ m/s and 4×800 g, $v_c = 0.53$ m/s). The given deformation of the physical model with 16×800 g weights at $v_c = 0.50$ m/s had obvious errors of unknown source in the deformed geometry measurements.

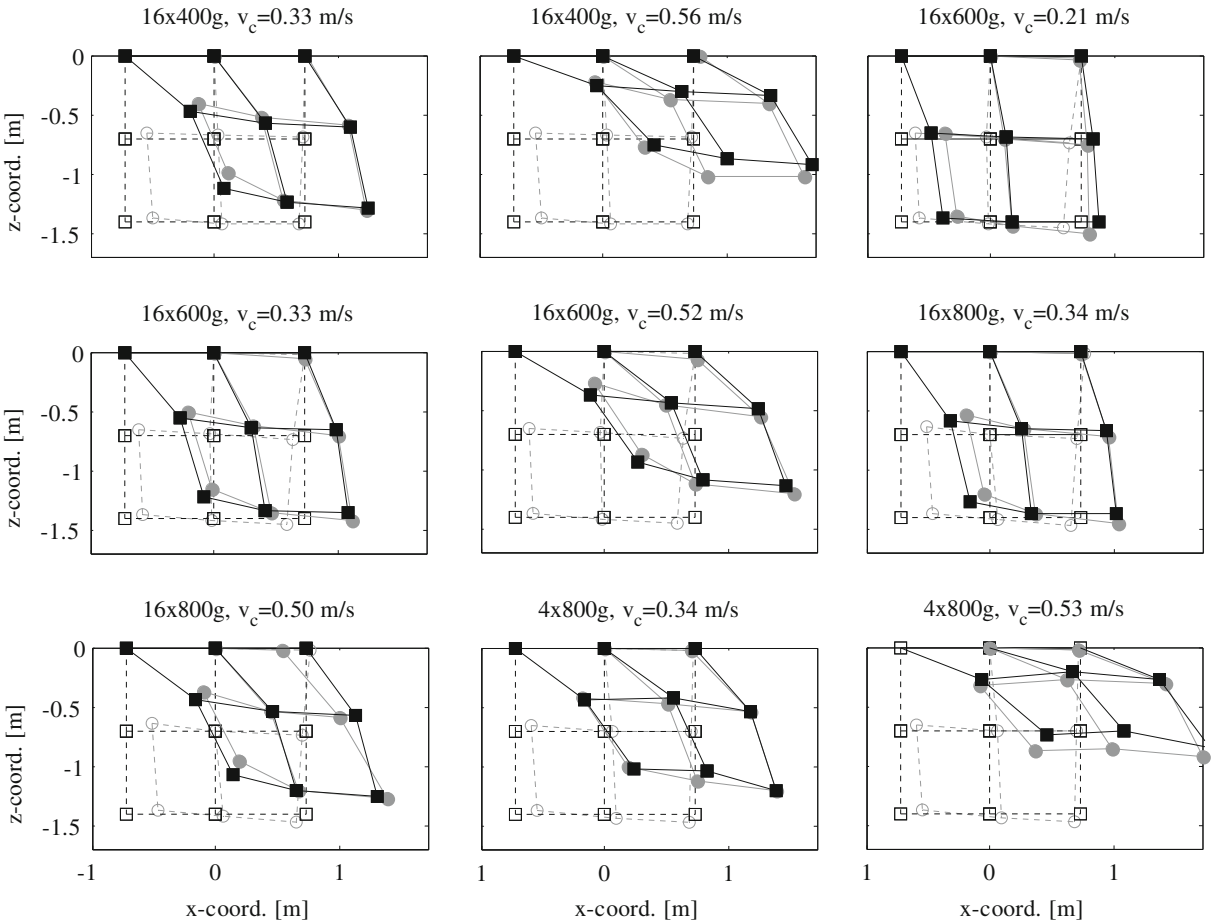

Fig. 5. Comparison of 2-D shape of net between physical model tests (given as grey circles) and numerical analysis (black squares). Shapes with and without current are given in all figures (filled markers for current).

The upper two points on the downstream side (right-hand side) was registered with an unlikely, probably too small, x-coordinate, while the bottom point may have a too large x-coordinate.

Figs. 6 and 7 give the resulting total drag and lift forces acting on M1 from model and numerical tests, and the volume reduction calculated based on the deformed numerical model. As would be expected, drag and lift forces increased with increased current velocity, while the volume decreased. Drag and relative volume seemed to be almost proportional with the current velocity for velocities above 0.2 m/s. There was good agreement in drag force, although the numerical analyses differed more in drag between the various bottom weights for high velocities, indicating that increased bottom weights increased the drag loads acting on the netting (due to reduced deformations). The results from the model tests indicated that there were significant uncertainties in the measured velocities and loads: the drag was measured to be slightly larger for a current velocity of 0.52 than 0.53, the opposite of what should be expected. In addition, the drag was measured to 0.7 N, while lift was 0.5 N in calm water (16×800 g weights).

The calculated drag force was $95 \pm 9\%$ of the measured values (mean and standard deviation), while the calculated total lift force was $83 \pm 10\%$ of the measured values (Fig. 7), disregarding a couple of the lower values of lift forces where the deviation probably was strongly affected by the mentioned uncertainties in load measurements. Even in the numerical analyses that showed a larger vertical deformation than model tests (Fig. 7), the lift forces were lower than the measured values.

The net cage volume was reduced close to proportional with increased current velocity (Fig. 6), resulting in a relative volume (volume in current divided by unloaded cage volume) of 30–63% for a current velocity of 0.5 m/s. Preservation of volume increased with increased bottom weights. Lader and Enerhaug (2005) estimated the relative volume based on

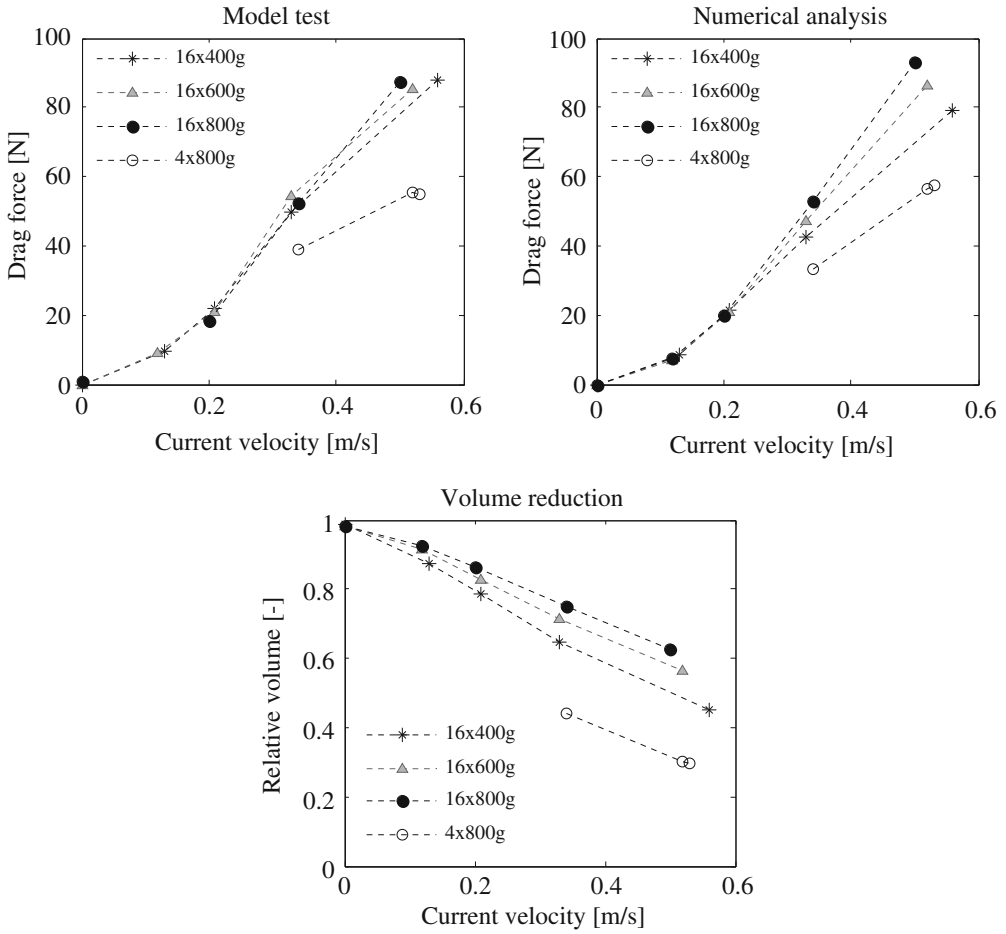

Fig. 6. Total drag force measured during model tests and calculated in numerical analysis of net cage M1. Relative volume in net cage M1 as a function of current velocity.

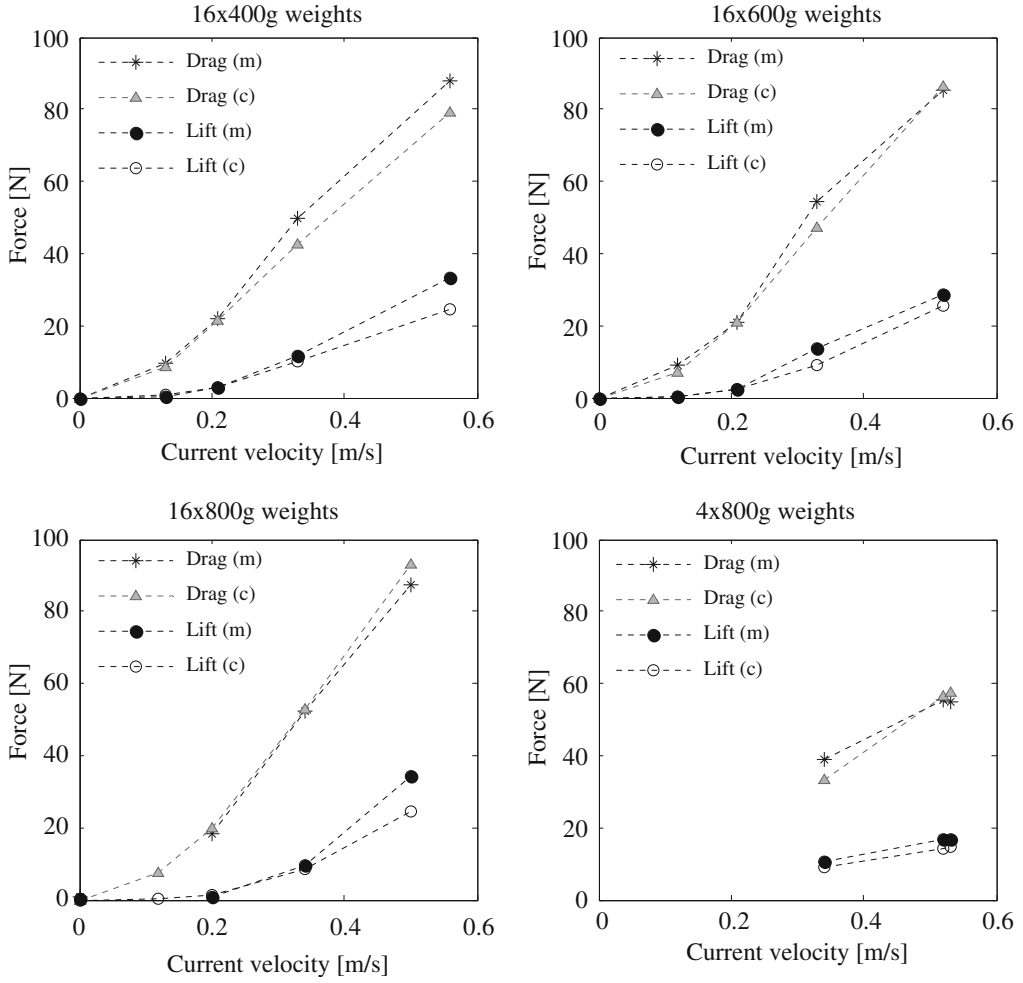

Fig. 7. Total drag and lift forces measured during model tests (m) and calculated in numerical analysis of net cage M1 (c) for the various weight configurations.

global deformation of the nets (Fig. 5), as a non-linear relationship between relative volume and current velocity. Their relative volume estimates gave larger values than the calculations presented in Fig. 6, probably because they were not able to include the effect of netting displacements on cage volume.

3.2. Strength analysis of full-scale net cages

Analyses of M1 showed that the numerical analysis corresponded reasonably well to the model test results. The method has thus been verified under the given conditions and corresponding numerical analyses can be performed on FE models of full-scale net cages. In addition to an evaluation of loads acting on the cage and their deformed shape, maximum values of local forces in the structure were found and compared to the design capacity (breaking strength divided by a material factor) of the various structural components.

The global results from analyses of M2 and M3 are given in Fig. 8. In general, drag loads increased with increased cage size, current velocity and bottom weights. For small velocities, an increase in drag force was approximately proportional to the velocity squared, as we would expect for negligible net cage deformations (according to Morison's equation). For larger velocities (>0.2 m/s), the deformation of the net cage resulted in a significant reduction in the normal velocity component ($|\mathbf{U}_N|$, Fig. 4) for some of the elements, compared to an undeformed net cage. The total resulting drag loads were almost proportional to the current velocity for velocities between 0.2 and 0.5 m/s. The lift forces increased with increased velocity, with varying rates of change.

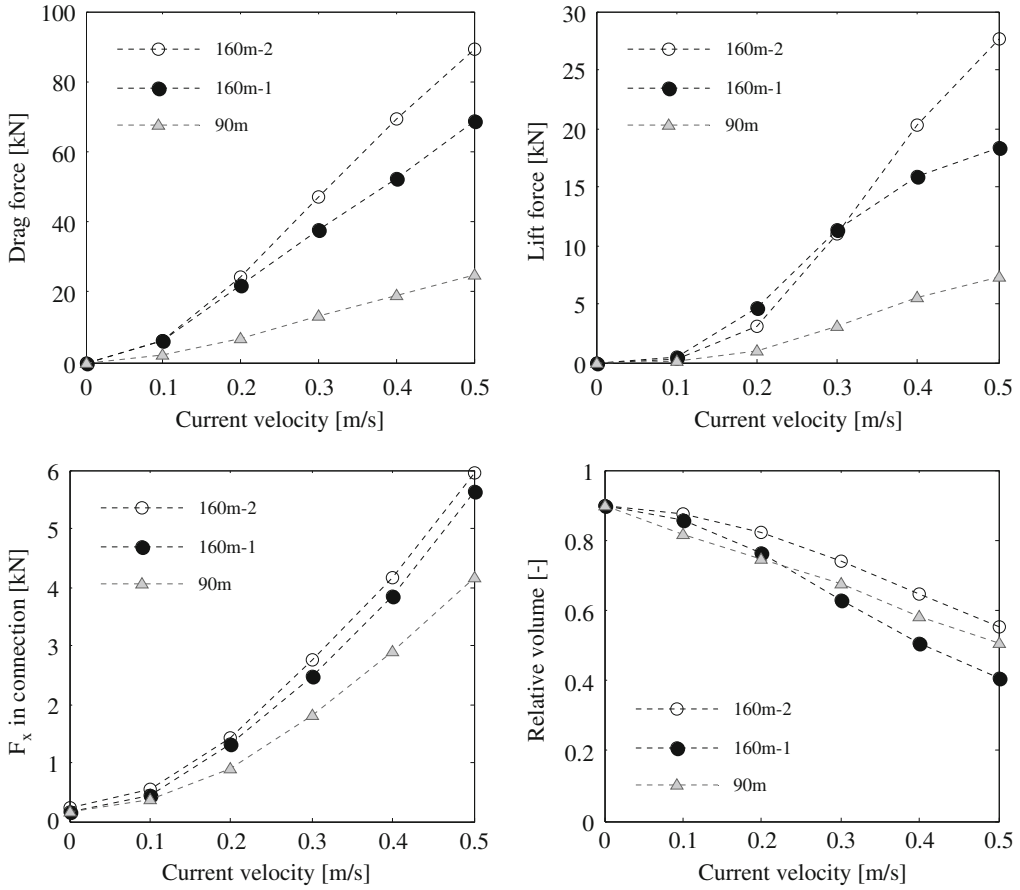

Fig. 8. Drag and lift forces, maximum forces in the x-direction in connection with cage collar and relative volume for M2 (90m) and M3 with 1000 N weights (160m−1) and 2000 N weights (160m−2).

Knowledge of the expected maximum forces acting in the connections between net cage and cage collar is important in designing and dimensioning of net cages. The connection point with the highest loads in the x- and z-directions was found in front of the cage (upper left point in Fig. 2). Loads in the x-direction, $\mathbf{F}_x$, for this point are given in Fig. 8. These horizontal connection forces increased with increase in velocity. The maximum connection force was not significantly affected by the increased bottom weights for M3, and not as sensitive to difference in cage size as the drag force. Loads in the z-direction, F_z did not vary much with current velocity for the full-scale models M2 (mean value and standard deviation of 1.2 ± 0.1) and M3 (mean value and standard deviation of 1.2 ± 0.1 for 1000 N weights and 2.1 ± 0.1 for 2000 N weights).

The relative volume of the net cages (Fig. 8) decreased with increase in current velocity, resulting in a value of 41–55% for a velocity of 0.5 m/s. The linear trend was not as clear in this figure as for M1. However, the volume for cages in currents less than 0.2–0.3 m/s was somewhat underestimated as the method for volume calculation did not consider the volume below the bottom rope of the cage. Fig. 9 shows the 2-D displacements of M3 with 1000 N weights, and how the central bottom weight increased the depth below the bottom rope of the cage significantly for velocities below 0.3 m/s. The net below the bottom rope formed a conical volume in calm water. Including this volume in the calculation of deformed cage volume gave a total relative volume of 1.0 in calm water. This indicated that the relationship between the total relative volume (including volume below the bottom rope) and current velocity had a linear trend for all net cages in Fig. 8.

Maximum forces in various structural components were found and are given for main ropes, side ropes, cross ropes, netting twines and seam in Fig. 10. In all components, the maximum forces increased with an increase in current velocity. In general the forces in net cage M2 were smaller than the forces in M3, except in the seam for low velocities. This is due to the low number of cross ropes in M2, increasing the stress concentration in the seam. Increasing the

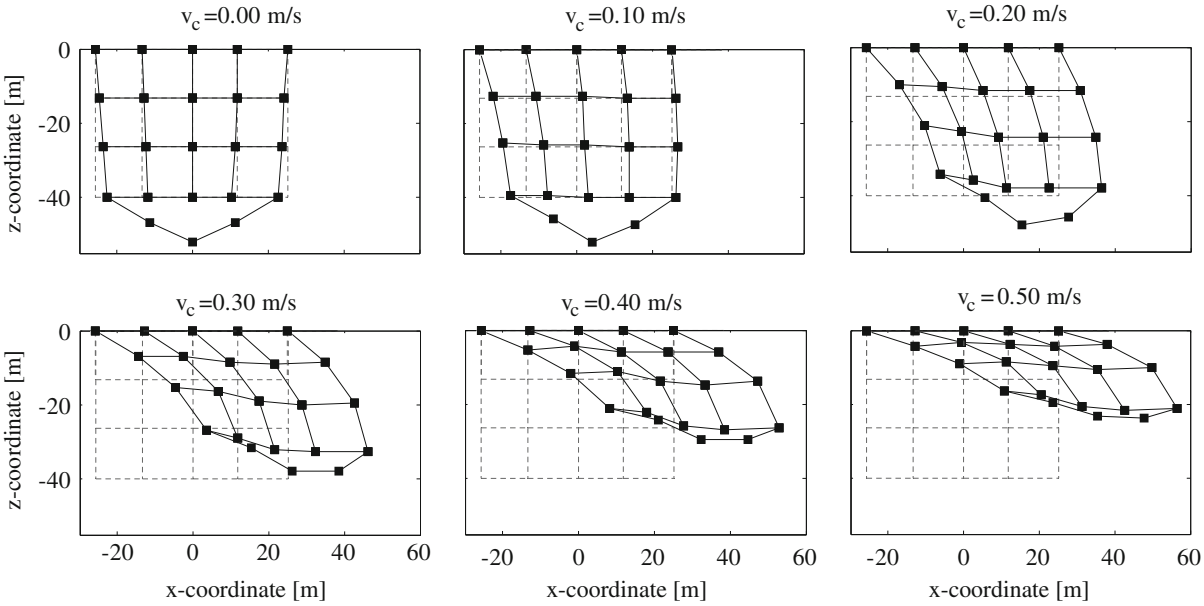

Fig. 9. Calculated 2-D net cage displacements for M3 with 1000 N weights in calm water and various current velocities. Undeformed cage configuration is given as dotted lines.

bottom weights only had a small effect on the local forces in the net cage, although the drag loads increased significantly (Fig. 8). The only significant deviation was in forces in side ropes, where the heavier weights naturally gave a higher tensile force in the side ropes, however the difference in force decreased between the two variations of M3 for increasing velocity.

The forces can be compared to the design capacity of the various structural components, using the following rule: the force in a component (F) multiplied by a load factor (γ_f) should be equal to or less than the capacity (R, i.e. breaking strength) of the component divided by a material factor (γ_m) (Standards Norway, 2003, 2004): $F\gamma_f \leq R/\gamma_m$. The percentage of utilized design capacity can be calculated as follows:

$$C_u = \frac{F\gamma_f\gamma_m}{R}, \tag{2}$$

based on NS9415 (Standards Norway, 2003), $\gamma_f = 1.3$ and $\gamma_m = 3$ for ropes, while no material factor was given for netting. Based on the results presented in Fig. 10, the maximum utilized design capacity for ropes was 20% for the main rope in M2, 31% for the main rope for M3 with 1000 N weights and 32% for the side rope for M3 with 2000 N weights. Forces in the netting twines were in general low (less than 9 N), considering that the breaking strength of each twine would be greater than 200 N for such netting dimensions (derived from NS9415). It is difficult to establish a material factor for netting, and this is consequently not given in NS9415. The seam was subjected to relatively high forces, up to 440 N for M3. If our assumption that the seam had 10 times the strength of a netting twine is valid, $C_u = 440 \times 1.3 \times \gamma_m/2000 = 0.29\gamma_m$, i.e. depending on the material factor we are close to or beyond utilizing the design capacity of the seam. One can also raise the question whether a component like a seam should be used as a load carrying member in a structure. Seams are known to be a problem area in the net cage, and it should be considered to increase the number of cross-ropes so that all load carrying points in the net are connected to a cross-rope in the bottom for circular cages, at least for large cages in intermediate to strong currents.

4. Discussion

Results from the numerical analyses corresponded well with the physical model tests. However, some deviations existed, especially in calculated lift forces which on average were 17% lower than the measured values. Several sources of error could have had significant effect on the model test results: the initial model geometry was imperfect, the current

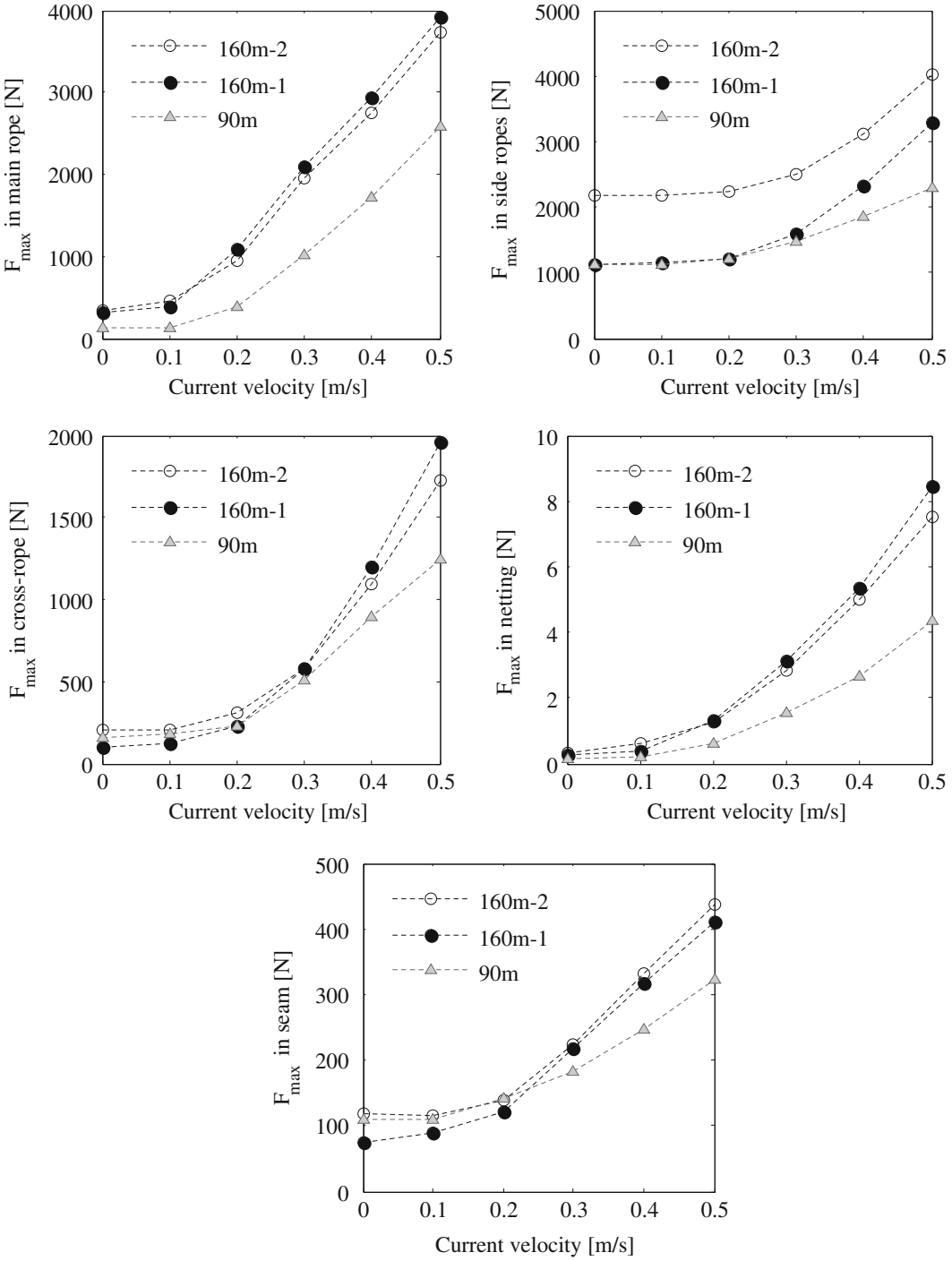

Fig. 10. Maximum calculated forces in structural component of net cage: Main rope, side ropes, netting seam in bottom and netting twines for M2 (90m) and M3 with 1000 N weights (160m−1) and 2000 N weights (160m−2).

velocity varied over the model depth and measurements of loads, current velocities and net configuration involved uncertainties (Enerhaug, 2003). In addition, the simplified numerical model did not give a perfect representation of the physical test: local dimensions of wet netting were estimated based on given dry dimensions (possible errors both in measurements of dry netting and estimation of wetting effect). The local netting geometry was not modelled in detail,

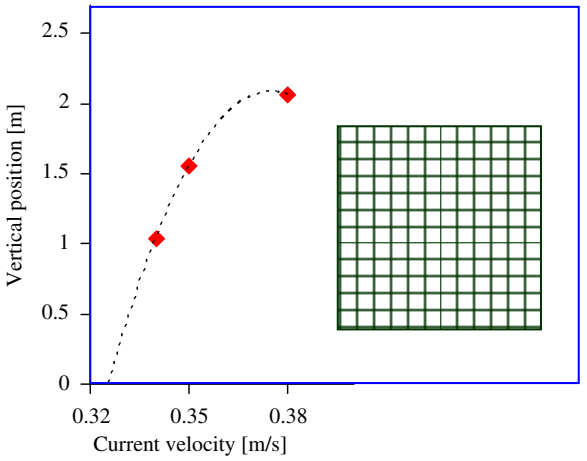

Fig. 11. Measurements of horizontal current velocity in 3 points over the depth of the flume tank (2.7 m) given by Enerhaug (2003). A current velocity trend and position and size of the undeformed net cage M1 are indicated.

but was modelled as a mesh of smooth cylinders. Drag calculations involved possible sources of error due to estimation of drag coefficients and shadow effects.

Measurements showed that the current velocity was not constant over the depth of the flume tank (Enerhaug, 2003, Fig. 11). The net cage was placed approximately 0.9 m below the water surface, and for one of the load cases the velocity was measured at three vertical positions as indicated in Fig. 11. Approximately 0.25 m above the cage, the velocity was 0.38 m/s, while 0.5 and 1.0 m below this point the velocity was reduced by approximately 8% and 11%. In the presented results (Figs. 5 and 7), the applied current velocity was measured in the intermediate point (1.4 m below the surface). The bottom of the net cage model M1 was lifted when the cage was subjected to loads from current (Fig. 5). A larger fraction of the net was thus subjected to the relative high velocities in the upper water levels. This may partly explain the deviation in lift forces for high velocities.

The velocity reduction in the centre of the net cage was given as 20% in Lader and Enerhaug (2005) (based on measurements from one of the load cases), although close studies of the velocity measurement from the tests indicate that the shadow effect may have been lower in the middle of the cage (Enerhaug, 2003). The velocity was measured in front of, in the middle and behind the net cage, and the data on velocity inside the full volume of the cage was thus unknown. Consequently, the shadow effect may not have been modelled accurately. A lower velocity reduction would probably increase both drag and lift loads.

It was not trivial to find suitable drag coefficients for the netting twines. An overview of data on drag coefficients for netting materials are given in Fredheim (2005), based on experiments performed on knotted netting materials by Rudi et al. (1988). Klebert (2009) have found that the drag coefficient may not be very different for knotless netting, and that the drag coefficient is close to constant for Reynolds numbers $\mathrm{Re} \in (300,1000)$, which corresponds to data from Rudi et al. (1988). A detailed study of drag coefficients was not included in this work. Based on data in Fredheim (2005) the given drag coefficient of 1.15 was chosen for the given solidity and velocities.

We conclude that the applied numerical model seems to reflect the results from the model tests as well as could be expected. However, more validation of the method is necessary. It should also be tested for larger current velocities, deformations and solidities. During large net cage deformations, significant fractions of the net cage will be affected by additional shadow effects where some of the twines will be positioned in the wake of one or several twines. The extreme example of this is a horizontal panel of netting (in the xy-plane) subjected to in plane current (in the x-direction). Using Morison's equation and the cross-flow principle, all elements with axis parallel to the y-axis will be subjected to a drag load proportional to the current velocity squared ($|\mathbf{U}|^2$), while the elements with axis parallel to the x-axis ($\alpha = 90^\circ$ in Fig. 4) will yield no drag load ($|\mathbf{U}_N| = 0$). Thus, we can assume that the drag calculated for a horizontal panel using Morison's equation is 50% less than for a vertical panel (in the yz-plane). According to results from model tests presented in Løland (1991), the drag of a horizontal panel is reduced by approximately 94% compared to a vertical panel. Thus, it must be assumed that drag loads can be overpredicted for large displacements if this potential shadow effect is not included. The applied method does not include this potential shadow effect. However, we do not see any effect of this in the presented results. In further analysis with even larger net cage deformations, this effect should be

considered when calculating the loads. During large net cage deformations, the tangential component of drag force could give a significant, although most likely small, contribution to the loads acting on the net cage.

The forces in the various structural components of the full-scale model were calculated for a geometrical perfect net cage model with perfectly applied loads and boundary conditions from a strength point of view. However, in practice all nets have imperfections like initial stress concentrations in the netting, variations in length of ropes and ends of side ropes and cross ropes that do not connect perfectly. This may introduce significantly larger forces in the netting than indicated in Fig. 10, and may also change the distribution of loads in the ropes with the possibility of increased maximum forces. This can be handled in the design process through introduction of increased load and material factors that include modelling uncertainties [γ_F and γ_M, Standards Norway (2004)]. Introducing a flexible cage collar with a significant deformation during loading would probably change the distribution of loads in the net cage, most likely increasing the maximum forces in side ropes and attachment loop.

Traditional knotless netting materials for aquaculture have a very low stiffness for small tensile loads. In fact, they are so flexible it is hard to define a precise initial length and stiffness. The actual stiffness of the applied netting materials may differ from the assumed 82 MPa. However, according to the numerical analyses, evenly distributed, moderate current loading will only introduce small strains in the netting of the analyzed cages. (The maximum nominal strain was 3% for M3 locally, while the major part of the net had strains less than 1%.) The ropes had a relatively large tensile stiffness, and errors in netting stiffness would not affect the loads in the netting or the deformed shape significantly (dominated by global displacement). In M1, strains in the netting were up to 3% in the twines above the weights, while most of the netting had strains less than 10^{-4}. The assumed value of 82 MPa represents the uniaxial stiffness of the netting materials, which can be applied for netting in net cages, as one load direction often dominates over the other for significant stress levels (Moe et al., 2007). The numerical analysis results showed that in the area with highest loads (upper part of the upstream side of the cage), the initially vertical twines were strained approximately 10 times as much as the initially horizontal elements.

5. Conclusions

This study indicated that finite element analyses can be applied to estimate deformations and loads acting on net cages. A method for structural analysis of aquaculture net cages was developed using a commercial FEA software and verified for a netting solidity of 0.23, water current velocities from 0.1 to 0.5 m/s and relatively large deformations (volume reduction up to 70%). Resulting drag loads were shown to be dependent on the net cage size and weight system, increasing close to proportional with the current velocity for velocities in the range 0.2–0.5 m/s. The corresponding lift forces increased with an increase in velocity, with varying rates of change. The cage volume was reduced almost proportionally with the current velocity.

The calculated forces in ropes and netting were well below the design capacity. However, the netting seams in the bottom panel of the net cage were identified as a potential problem area as the forces could reach the design capacity.

Acknowledgements

This work was funded by the Norwegian Research Council through the research programmes IntelliSTRUCT (Intelligent Structures in Fisheries and Aquaculture) at SINTEF Fisheries and Aquaculture and SECURE (Securing fish-farming technology and operations to reduce escapes). We would like to thank Birger Enerhaug, Østen Jensen, Martin Føre and Pål Lader at SINTEF Fisheries and Aquaculture for their help and good advice during this work.

References

Dessault Systèmes, 2007. ABAQUS 6.7 Documentation.

Enerhaug, B., 2003. Model Tests of Net Structures. SINTEF Report.

Enerhaug, B., Lader, P., 2009. Unpublished Data.

Fredheim, A., 2005. Current forces on net structures. Doctoral Thesis (Dr. Eng.), Norwegian University of Science and Technology, Norway.

Faltinsen, O.M., 1990. Sea Loads on Offshore Structures. Cambridge University Press, Cambridge Ocean Technology Series.

Gignoux, H., Messier, R.H., 1999. Computational modelling for fin-fish aquaculture net pens. Oceanic Engineering International 3, 12–22.

Hoerner, S.F., 1965. Fluid-Dynamic Drag. Hoerner Fluid Dynamics.
Huang, C.-C., Tang, H.-J., Liu, J.-Y., 2006. Dynamical analysis of net cage structures for marine aquaculture: numerical simulation and model testing. Aquacultural Engineering 35, 258–270.
Klebert, 2009. Unpublished Data.
Klust, Gerhard, 1982. Netting Materials for Fishing Gear. Fishing News Books Ltd., England.
Lader, P., Enerhaug, B., 2005. Experimental investigation of forces and geometry of a net cage in uniform flow. IEEE Journal of Ocean Engineering 30, 79–84.
Lader, P.F., Fredheim, A., 2006. Dynamic properties of a flexible net sheet in waves and current—a numerical approach. Aquacultural Engineering 35, 228–238.
Li, Y.-C., Zhao, Y.-P., Gui, F.-K., Teng, B., 2006. Numerical simulation of the hydrodynamic behaviour of submerged plane nets in current. Ocean Engineering 33, 2352–2368.
Løland, G., 1991. Current forces on flow through fish farms. Doctoral Thesis (Dr. Eng.). The Norwegian Institute of Technology, Norway.
Moe, H., Fredheim, A., Heide, M., 2005. New Net Cage Designs to Prevent Tearing During Handling. IMAM 2005, Lisbon, Portugal, 26–30 September 2005.
Moe, H., Olsen, A., Hopperstad, O.S., Jensen, Ø., Fredheim, A., 2007. Tensile properties for netting materials used in aquaculture net cages. Aquacultural Engineering 37, 252–265.
Moe, H., Hopperstad, O.S., Olsen, A., Jensen, Ø., Fredheim, A., 2009. Temporary creep and post creep properties of aquaculture netting materials. Ocean Engineering 36, 992–1002.
Priour, D., 1999. Calculation of net shapes by the finite element method with triangular elements. Communications in Numerical Methods in Engineering 15, 755–763.
Rudi, H., Løland, G., et al., 1988. Experiments with Nets; Forces on and Flow Through Net Panels and Cage Systems. SINTEF Report.
Standards Norway, 2004. NS 3490 Design of Structures—Requirements to Reliability.
Standards Norway, 2003. NS 9415 Marine Fish Farms—Requirements for Design, Dimensioning, Production, Installation and Operation.
The International Organization for Standardization, 2002. ISO 1107 Fishing Nets – Netting – Basic Terms and Definitions.
Tsukrov, I., Eroshkin, O., Fredriksson, D., Swift, M.R., Celikkol, B., 2003. Finite element modelling of net panels using a consistent net element. Ocean Engineering 30, 251–270.
Tronstad, H., 2000. Nonlinear hydroelastic analysis and design of cable net structures like fishing gear based on the finite element method. Doctoral Thesis (Dr. Eng.), The Norwegian University of Science and Technology, Norway.
Zhan, J.M., Jia, X.P., Li, Y.S., Sun, M.G., Guo, G.X., Hu, Y.Z., 2006. Analytical and experimental investigation of drag on nets of fish cages. Aquacultural Engineering 35, 91–101.
Zhao, Y.-P., Li, Y.-C., Dong, G.-H., Gui, F.-K., Teng, B., 2007. Numerical simulation of the effects of structure size ratio and mesh type on three-dimensional deformation of the fishing-net gravity cage in current. Aquacultural Engineering 36, 285–301.